Adsorption Characteristics of Trace Volatile Organic Compounds in Gas Streams onto Activated Carbon Fibers

K. L. Foster,† R. G. Fuerman,‡ J. Economy,*,† S. M. Larson,‡ and M. J. Rood‡

Department of Materials Science and Engineering and Department of Civil Engineering, University of Illinois, 1304 W. Green St., Urbana, Illinois 61801

Received April 17, 1992. Revised Manuscript Received June 26, 1992

The adsorption characterstics of activated carbon fibers (ACF) prepared from phenolic precursors were examined. Three ACF with specific surface areas of 900, 1610, and 2420 m^2/g were used to determine the adsorption of volatile organic compounds (VOC) over a range of concentrations in air or nitrogen gas streams. Gravimetric adsorption was used both to determine the ACF effective pore volume using several individual VOC saturated in nitrogen or air at atmospheric pressure and to determine adsorption isotherms of *n*-butane over a large range of concentrations (49.8 ppmv to 99.5 vol %) in nitrogen at atmospheric pressure and 25 °C. The experimental results showed that while for saturated adsorption results, where adsorption increased with increasing ACF specific surface area, at lower concentrations the ACF with the least specific surface area adsorbed more. This low concentration reversal was also observed with acetone (10.3 ppmv) in air and benzene (56.5 ppmv) in nitrogen. We conclude that this isotherm crossover results from the ACF activation process where the micropores are widened (and the specific surface area concomitantly increased) with increasing activation duration and that this crossover is in agreement with predictions of the Dubinin–Radushkevich equation. These results are important for the development and design of materials for low concentration adsorption applications such as maintaining and improving ambient air quality.

Introduction

Volatile organic compounds (VOC), often present in ambient air at 1 ppbv to 1000 ppmv (parts per million based on volume) concentrations,[1,2] may contribute to a variety of physical symptoms, such as headaches, nausea, and dizziness.[3,4] Such symptoms have been reported among workers in office environments, resulting in an increased awareness of health problems attributed to poor ambient air quality. VOC consist of aromatic compounds such as toluene or benzene as well as many aliphatic compounds such as *n*-hexane or 2-methylbutane. Several studies[5,6] have determined typical levels of VOC found in actual building air systems and have generally depended on increased ventilation and/or reducing the source emissions to reduce concentrations of VOC. Another method to consider is the removal of VOC from gas streams by adsorption with activated carbon.

Adsorption of organic gases onto activated carbon is not new. Ample literature[7-11] describes the preparation, adsorption, and structural properties of activated carbons. These carbons have a large specific surface area resulting in high adsorption capacity. Although amorphous, activated carbons have a structure consisting of layers of twisted ribbonlike defective graphite planes. The narrow space between sets of graphite planes is often no larger than 2 nm and can extend down to molecular dimensions as demonstrated by carbon-based molecular sieves.[12-14]

Activated carbons have a measurable micropore(<2 nm)[15] volume which is denoted as the effective pore volume.[16] This nomenclature acknowledges that the size of different molecular probes, their packing in the micropores, and their interactions with carbon can result in different measured micropore volumes for each probe.

Micropores, rather than the larger macro- and mesopores, are preferentially filled at low relative pressures (adsorbate pressure/saturated adsorbate pressure) due to the overlap of attractive forces of opposite pore walls.[7] Within wider pores, attractive forces of opposite pore walls overlap less, effectively lowering the amount of adsorption occurring at low relative pressures in comparison to the adsorption within the micropores. In a like manner, micropores are primarily responsible for adsorption at low concentrations (ppbv and ppmv) in ambient air environments. It is this preferential filling of the micropores that we wish to explore as a means to optimize adsorption of VOC onto activated carbons. Applications of this research include development of activated carbons as the basis of a control technology designed to maintain and to improve ambient air quality.

Economy and Lin[17,18] have demonstrated the preparation and adsorption properties of phenolic based activated carbon fibers (ACF). ACF are commercially available from Nippon Kynol Inc. in three different degrees of activation and are prepared by direct activation of a cross-linked

† Department of Materials Science and Engineering.
‡ Department of Civil Engineering.
* To whom correspondence should be sent.

(1) Spengler, J. D.; Sexton, K. *Science* **1983**, *221*, 9.
(2) Fuerman, R. G.; Cal, M. P.; Larson, S. M.; Rood, M. 84th Annual Meeting and Exhibition, Vancouver, British Columbia, June 16-21, 91-62.5, 1991.
(3) MacFarland, H. N. *Am. Ind. Hyg. Assoc. J.* **1986**, *47*, 704.
(4) Tancrede, M.; Wilson, R.; Zeise, L.; Crouch, E. A. C. *Atmos. Environ.* **1987**, *21*, No. 10, 2187.
(5) Hodgson, A. T.; Daisey, J. M.; Grot, R. A. *J. Air Waste Manage. Assoc.* **1991**, *41*, 1461.
(6) Sheldon, L. S.; Zelon, H.; Sickles, J.; Eaton, C.; Hartwell, T.; Jungers, R. 81st Annual Meeting of APCA, Dallas, TX, June 19-24, 1988.
(7) Gregg, S. J.; Sing, K. S. W. *Adsorption, Surface Area and Porosity*, 2nd ed.; Academic Press: London, 1982.
(8) Rodríguez-Reinoso, F.; Garrido, J.; Martín-Martínez, J. M.; Molina-Sabio, M.; Torregrosa, R. *Carbon* **1989**, *27*, 23.
(9) Walker, P. L., Jr. *Carbon* **1990**, *28*, 261.
(10) McEnaney, B. *Carbon* **1987**, *25*, 49.
(11) Dubinin, M. M. *Progress in Surface and Membrane Science*; Cadenhead, D. A., Danielli, J. F., Rosenberg, M. D., Eds.; Academic Press: 1975; Vol. 9.
(12) Lamond, T. G.; Metcalfe, J. E., III; Walker, P. L., Jr. *Carbon* **1965**, *3*, 59.
(13) Moore, S. V.; Trimm, D. L. *Carbon* **1977**, *15*, 177.
(14) Vyas, S. N.; Patwarthan, S. R.; Natraj, H. B. *J. Chem. Soc., Faraday Trans.* **1990**, *86* (20), 3455.
(15) Sing, K. S. W.; Everett, D. H.; Haul, L. Moscou, R. A. W.; Pierotti, R. A.; Rouqueril, J.; Siemienewska, T. *Pure Appl. Chem.* **1985**, *57*, 603.
(16) Sing, K. S. W. *Carbon* **1989**, *27*, 5.
(17) Lin, R. Y.; Economy, J. *Appl. Polym. Symp.* **1973**, *21*, 143.
(18) Economy, J.; Lin, R. Y. *Appl. Polym. Symp.* **1976**, *29*, 199.

0897-4756/92/2804-1068$03.00/0

phenol–aldehyde fiber at 800–1000 °C using the products of combustion of liquified petroleum gas and air.[19] The phenolic fiber precursor can be woven into a wide range of textile forms before activation. On the basis of molecular probe measurements,[20] ACF are microporous with slit-shaped pores similar to those observed with other activated carbons.[21,22] The ACF have the advantage of in situ electrical reactivation and greater rates of adsorption over conventional granulated activated carbons.[17,18]

In this paper we take advantage of the different pore structures available with increased activation and describe the evaluation of ACFs for use in the adsorption of VOC from a gas phase. Experimental results are presented describing the adsorption of *n*-butane, acetone, and benzene onto ACF at various concentrations (10 ppmv to 99.5%) at 25 °C. An unusual crossover in adsorption capacity with concentration is reported here for the first time. These results are compared qualitatively with the predictions of the Dubinin–Radushkevich[11] equation for three model fibers.

Experimental Section

ACF were obtained from American Knyol, Inc. (New York) with three different specific surface areas. The first is ACC-5092-15 and is denoted as ACF-15. The second and third are ACC-5092-20 (ACF-20) and ACC-509-25 (ACF-25). The three ACF were similarly prepared in a proprietary process from a woven phenolic precursor with the same activation gases at similar temperatures but with increasing activation durations to achieve increasing specific surface area. Here ACF-15 has the lowest specific surface area and ACF-25 has the highest. The ACF were characterized with the Brunauer, Emmett, and Teller (BET) method,[7] scanning electron microscopy (SEM), elemental analysis, X-ray photoelectron spectroscopy (XPS), and saturated gas adsorption of several VOC. Results from these tests are presented below.

Although adsorption experiments are often performed under vacuum, we have examined the adsorption of VOC onto ACF in air or nitrogen at atmospheric pressure. This more closely simulates the adsorption environment experienced by VOC in ambient air. At room temperature even low boiling point gases, like nitrogen, will adsorb to activated carbons[23] occupying some of the available pore volume. This may influence the adsorption of VOC by blocking or reducing their access to micropores.

The adsorption of gases was characterized by a gravimetric method using a TGA 951 (TA Instruments, New Castle, DE) interfaced with a TA Instruments 2100 system computer. The TGA-951 is a horizontal balance with a side arm quartz tube surrounding a platinum pan and quartz balance arm. The horizontal design minimizes the effects of gas flow rates on the pan that are often experienced with vertical designs. A small ceramic heater is located around the quartz tube and is controlled to 25 ● 0.2 °C. The TGA-951 is located on a balance table to minimize vibrations and increase stability. A gas flow rate of 60 mL/min was controlled with standard rotometers (Linde FM 4601-1111). In some experiments two mass flow controllers (FC-280) by Tylan General (Torrance, CA) were used to dilute a standard gas concentration to a lower concentration.

The certified standard gases used in the experiments were certified for concentration and obtained through Matheson, Inc. The *n*-butane in ultrahigh-purity (UHP) nitrogen was obtained in 95.8 ppmv, 968 ppmv, 1.01 vol % (percent by volume), and 9.88 vol % concentrations. In addition research grade 99.5% *n*-butane was obtained. The concentration of benzene was 56.5 ppmv in UHP nitrogen and the acetone was 10.3 ppmv in hydrocarbon free air.

Table I. Specific Surface Area and Elemental Composition of ACF Samples[a]

ACF	surface area[b]	C (wt%)	H (wt%)	O (wt%)
ACF-15	900	92.8	1.04	6.12
ACF-20	1610	95.4	0.68	3.92
ACF-25	2420	95.4	0.59	3.97

[a] All samples had <0.05% nitrogen. [b] BET specific surface area (m^2/g).

All ACF samples were initially dried in the TGA-951 with UHP nitrogen at 120 °C for 60 min before cooling to 25 °C. After an equilibration time of several hours at 25 °C the inlet line was switched over to the gas mixture and the mass change of the sample was recorded with time until equilibrium had been reached. This equilibrium time was dependent on the concentration of VOC in the gas and the adsorption characteristics of the fiber. Sample equilibration times as long as 7000 min were needed for some of the lowest concentrations (10 ppmv acetone).

The surface area of the sample was determined with a Micromeritics (Norcross, GA) ASAP 2400 using nitrogen at liquid nitrogen temperatures. The surface area was determined from the calculation of a monolayer using the BET equation in the relative pressure range 0.01–0.25.

The effective pore volumes of the ACF samples were determined by measuring the mass of adsorbed organic material at equilibrium conditions in saturated gas streams with the TGA-951 at 25 °C. All ACF samples were initially dried in the TGA-951 with UHP nitrogen at 120 °C for 60 min before cooling to 25 °C. After an equilibration time of several hours at 25 °C the inlet line was switched over to a gas stream saturated with acetone, benzene, cyclohexane, toluene, or 1,1,1-trichloroethane and the mass change of the sample was recorded with time until equilibrium had been reached. The adsorbates were assumed to condense in the pores and the effective pore volume was determined by converting the mass of the adsorbed adsorbate to a liquid volume using the adsorbate's liquid density. The saturated gas streams were prepared by bubbling nitrogen at 60 mL/min through the liquid of interest at room temperature.

Elemental analysis was used to determine the amount of carbon, hydrogen and nitrogen in the virgin ACF sample using a combustion tube technique.[24] A Model 240XA elemental analyzer (Control Equipment Corp.) was used to characterize the amounts of carbon, hydrogen, and nitrogen in the ACF. Oxygen was determined by mass difference assuming the ACF consisted only of carbon, hydrogen, nitrogen, and oxygen.

XPS analysis was used to verify the oxygen content on the ACF surface and also to describe the functional groups on the surface.[25–27] This was carried out with a PHI 5400 (Perkin-Elmer Corp., PE Div., Eden Prairie, MN). A magnesium anode and a spot size of 3 mm were used. XPS analysis requires the sample to be placed in ultrahigh vacuum; thus, the ACF samples were dried at 120 °C for 2 days to remove volatiles adsorbed before being placed in the XPS chamber.

Results and Discussion

The measured specific surface areas of ACF-15, ACF-20, and ACF-25 fibers were 900, 1610, and 2420 m^2/g, respectively, with each ACF exhibiting a type I isotherm typical of microporous materials. Only ACF-25 showed a trace amount of desorption hysteresis, indicating some mesopore character. Increased ACF specific surface area is obtained by activating the fibers under the same conditions[17,19] but for a greater duration. The specific surface area results are summarized in Table I, along with the results from the elemental analysis.

(19) Kasaoka, S.; Sakata, Y.; Tanaka, E.; Naitoh, R. *Int. Chem. Eng.* **1989**, *29*, 101.
(20) Kasaoka, S.; Sakata, Y.; Tanaka, E.; Naitoh, R. *Int. Chem. Eng.* **1989**, *29*, 734.
(21) McEnaney, B. *Carbon* **1988**, *26*, 267.
(22) Sing, K. S. W. *Carbon* **1989**, *27*, 5.
(23) Meredith, J. M.; Plank, C. A. *J. Chem. Eng. Data* **1967**, *12*, 259.
(24) Skoog, D. A.; West, D. M. *Fundamentals of Analytical Chemistry*, 4th ed.; CBS College Publishing: 1982; pp 629–632.
(25) Gai, P. L.; Billinge, B. H. M.; Brown, A. M. *Carbon* **1989**, *27*, 41.
(26) Salvati, L. T., Jr.; Hook, J.; Gardella, J. A., Jr.; Chin, R. L. *Polym. Eng. Sci.* **1987**, *27*, 13.
(27) Briggs, D.; Seah, M. P. *Practical Surface Analysis by Auger and X-ray Photoelectron Spectroscopy*; John Wiley & Sons: New York, 1983.

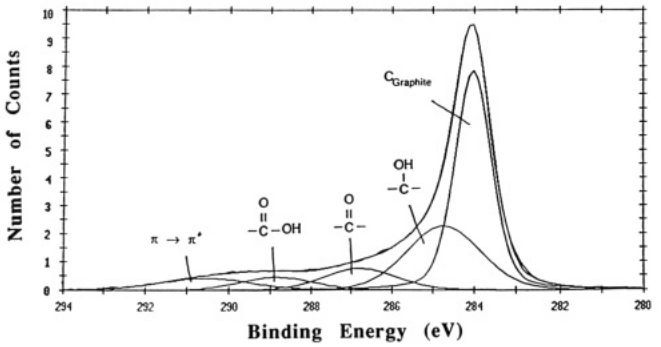

Figure 1. XPS spectrum of ACF-20 showing the deconvolution of the main spectral line into its functional components.

Table II. XPS Deconvolution of the Carbon 1s Peak Area[a]

ACF	carbon (graphite)	hydroxyl	quinone	carboxylic
ACF-15	46.0	33.5	10.3	4.1
ACF-20	50.9	27.9	9.3	5.6
ACF-25	54.7	24.4	8.4	5.7

[a] Percent by mass of total carbon existing in a particular form.

Table III. Comparison of Carbon/Oxygen Mass Ratios with XPS and Elemental Analysis

ACF	C/O (XPS)	C/O (elemental)
ACF-15	19.0	15.2
ACF-20	23.8	24.3
ACF-25	27.3	24.0

Elemental analysis revealed the ACF are greater than 92% by mass carbon with less than 1% by mass hydrogen and no nitrogen. The remainder is assumed to be oxygen and is present at 4–6% by mass and exists as quinones, phenols, and carboxylic acid groups.

XPS allows us to determine the elemental composition on the surface of the ACF. XPS experiments with these fibers found two peaks at 284 eV (C_{1s}) and 534 eV (O_{1s}). The carbon signal, shown in a spectrum of ACF-20 (Figure 1), allows us to determine the ratio of carbon-based functional groups. It has a broad asymmetric shape extending from 282 to 294 eV, indicating several carbon species of different binding energies. This signal was deconvoluted, suggesting three functional groups[28] shifted from the main carbon line at 284 eV. The area of Gaussian fit to these shifts at 284.0 (hydrocarbon), 284.7 (hydroxyl), 286.8 (carbonyl), and 288.8 eV (carboxyl) represents the relative amount of these functional groups. The peak at 290.5 eV is due to a π-electron cloud often observed in graphite. Only 5.6% by mass of the carbon exists as carboxyl, 9.3% by mass as quinone, and 27.9% mass as hydroxyl. Similar results were obtained for all three fibers as summarized in Table II. Similar surface functional groups on all three fibers suggests that the chemical properties and thus their chemical interactions with VOC should be similar.

The oxygen signal shows that the oxygen does not lie only on the surface of the fiber but throughout the entire fiber. This is shown by comparing the XPS results with the combustion tube elemental results. XPS is a surface analysis technique and is limited to the depths of only 30–100 Å below the fibers' surface[27] while the combustion tube technique determines the elemental composition of the entire fiber. The carbon to oxygen ratio of the XPS

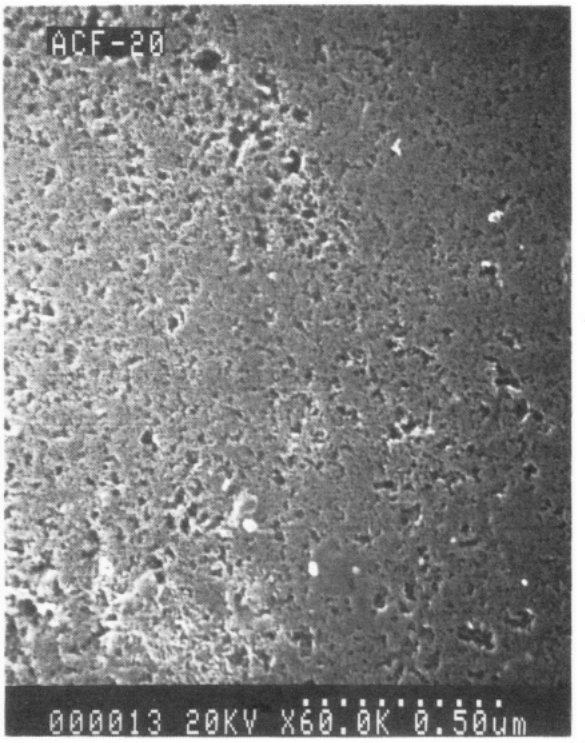

Figure 2. SEM image of the outside of an ACF-20 fiber (60X enlargement).

Table IV. Effective Pore Volume for Select VOCs

adsorbate	adsorbent (vol adsorbed cm^3/g) ACF-15	ACF-20	ACF-25
acetone	0.326	0.613	0.859
cyclohexane	0.314	0.638	0.805
benzene	0.323	0.653	0.849
toluene	0.345	0.632	0.877
1,1,1-trichloroethane	0.319	0.643	0.834
mean pore vol[a]	0.325	0.636	0.845
std dev	0.012	0.015	0.027

[a] cm^3 of adsorbate/g of ACF at 25 °C.

results (Table III) agree with the previous elemental results obtained using the combustion tube technique. This agreement with the carbon to oxygen ratios between the elemental analysis and XPS suggests that oxygen is uniformly distributed across the diameter of the fiber.

The fibers were examined with SEM to determine the effects that longer activation times might have on surface topography. The outside surface of a typical ACF-20 fiber is shown in Figure 2. It shows a smooth surface with numerous intrusions up to 500 Å. These intrusions may serve as transition pores and have been reported to increase the rate of adsorption of activated carbons by allowing the gas to more quickly reach micropores located in the interior of the fiber.[29] These intrusions were confirmed with neutron scattering.[30] We were not able to discern any difference in surface appearance between the three ACF within the limits of SEM resolution available.

The effective pore volume (cm^3 of adsorbate/g of ACF) was measured for each ACF with a series of VOC and found to increase with increasing duration of activation correlating well with the effective surface area. ACF-25 had the greatest effective pore volume followed next by ACF-20 and finally ACF-15. Table IV shows a mean ef-

(28) Wagner, C. D.; Riggs, W. M.; Davis, L. E.; Molder, J. S.; Muilenberg, G. E. *Handbook of Photoelectron Spectroscopy*; Perkin-Elmer, Physical Electronics Division: Eden Prairie, MN, 1979.

(29) Hayes, J. S., Jr. *Novoloid Nonwovens*; Nonwoven Symposium, April 1985, TAPPI Press, Atlanta, GA.

(30) Kieffer, J. Investigations of the Transitional Pore Structure of Activated Carbon Fibers by SANS. Submitted to *J. Appl. Phys.*

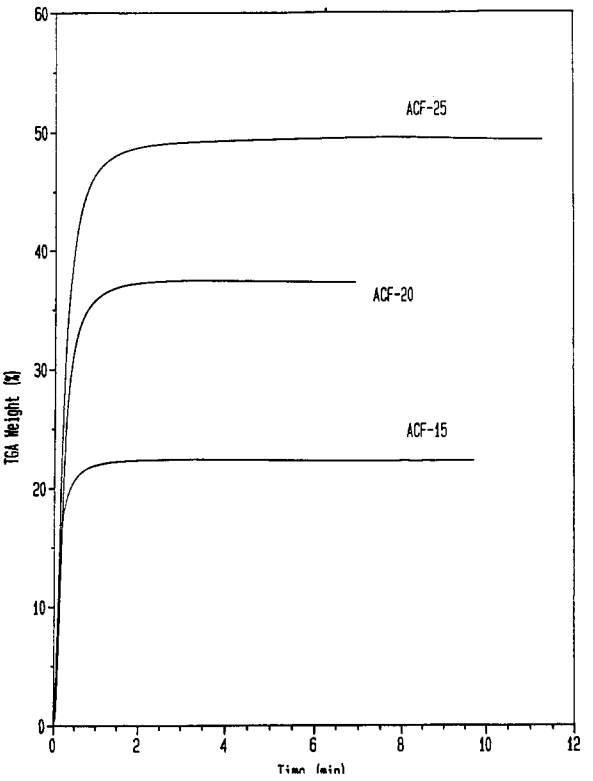

Figure 3. Weight gain of ACF at 99.5% *n*-butane.

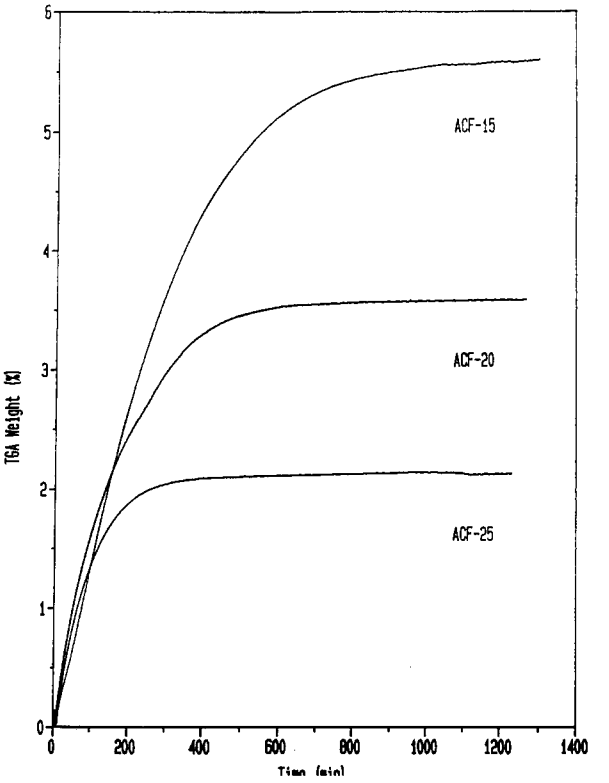

Figure 4. Weight gain of ACF at 95.8 ppmv *n*-butane in nitrogen.

fective pore volume of 0.325 cm^3/g for ACF-15 with a standard deviation of 0.012 cm^3/g. The mean effective pore volume for ACF-20 was 0.636 cm^3/g and for ACF-25 it was 0.845 cm^3/g with standard deviations of 0.015 and 0.027 cm^3/g, respectively. The similarity between volume adsorbed onto each ACF for differing adsorbates is consistent with the Gurvitsch rule[31] indicating that different adsorbates adsorb onto an adsorbent with the same liquid volume. Note the Gurvitsch rule is not necessarily followed when adsorbates of large dimension are used compared to the pore dimensions.

Gas adsorption experiments yielded the most surprising results. When a 99.5 vol % concentration of *n*-butane in nitrogen was used, the fibers adsorbed as expected with ACF-25 adsorbing the greatest amount of *n*-butane and ACF-15 adsorbing the least, consistent with the trend of increasing effective pore volume for ACF samples of increasing specific surface areas. A set of typical gas adsorption results are shown in Figure 3 where ACF-25 adsorbs 49.8 wt %, ACF-20 adsorbs 37.1 wt %, and ACF-15 adsorbs 22.9 wt % of *n*-butane at equilibrium.

On the other hand at lower adsorbate concentrations, we observed a reverse of the correlation with specific surface area. Thus for 95.8 ppmv *n*-butane (Figure 4) a complete reversal in adsorption is observed compared to adsorption behavior of 99.5 vol % *n*-butane. Here, at equilibrium, ACF-15 adsorbs the most at 5.6 wt %, ACF-20 adsorbs 3.6 wt %, and ACF-25 is lowest at 2.1 wt %.

A summary of the *n*-butane adsorption isotherm on ACF for a range of *n*-butane concentrations from 48.3 ppmv to 99.5% *n*-butane is shown in Figure 5. There are several features to note on this log–log plot. The most important is the crossover point observed near 5000 ppmv. Below this crossover point the ACF-15 is the greatest adsorber, but above this point the ACF-15 adsorption remains nearly constant while ACF-20 and ACF-25 adsorption continues to increase with concentration.

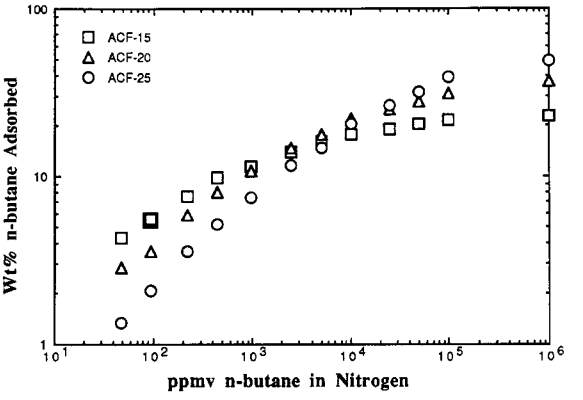

Figure 5. Adsorption isotherm of *n*-butane on activated carbon fibers.

As demonstrated in the effective pore volume determinations for a series of ACF samples previously, the adsorption of acetone saturated air and benzene saturated nitrogen also followed the correlation of increasing equilibrium adsorption with increasing effective surface area of the adsorbent. But, again, the amount of adsorbate adsorbed at equilibrium with low concentration gas streams of benzene or acetone decreased with increasing effective surface area. This low concentration adsorption reversal of the three ACF were examined using a 56.6 ppmv benzene in nitrogen and 10.3 ppmv acetone in air (Figures 6 and 7, respectively). In both cases the ACF-15 adsorbed more adsorbate than ACF-20, which in turn adsorbed more adsorbate than ACF-25.

The location of the crossover point and the amount of equilibrium adsorption at high concentrations are clearly dependent on the pore size distribution and the total available pore volume. The high concentration adsorption is dependent primarily on the total available pore volume and is demonstrated by ACF-15 reaching capacity at lower concentrations than the other two ACFs. The behavior at lower concentrations requires more explanation. Since

(31) Gurvitsch, L. *J. Phys. Chem. Soc. Russ.* **1915**, *47*, 805.

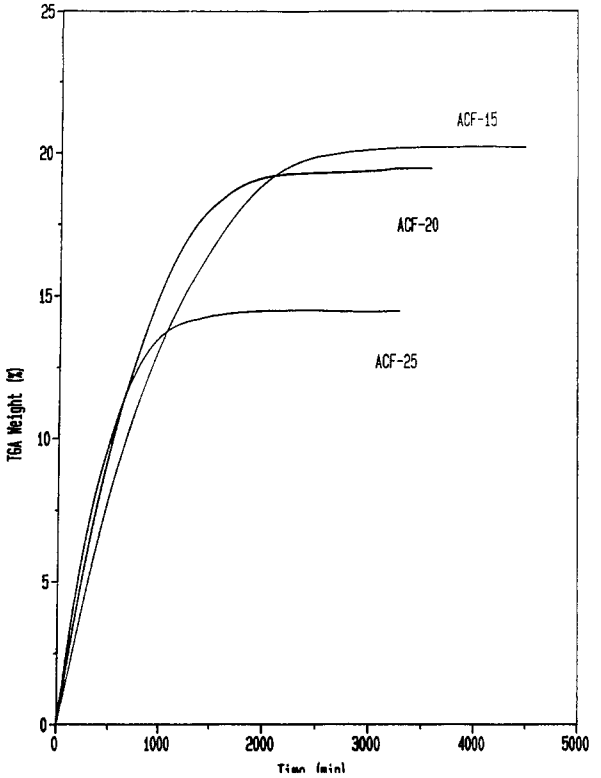

Figure 6. Weight gain of ACF at 56.6 ppmv benzene.

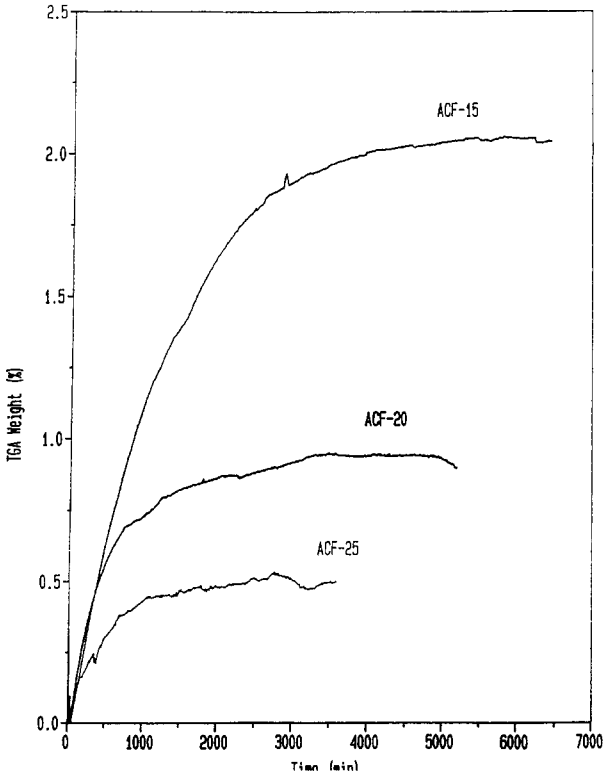

Figure 7. Weight gain of ACF at 10.3 ppmv acetone.

the fibers have similar chemical and external surface characteristics the preferential filling of micropores represents the most likely explanation of the low concentration isotherm reversal. If preferential micropore filling at low adsorbate concentration is indeed occurring with the smallest pore sizes filling first, as is generally believed,[7,11] and since the more activated surfaces adsorb less adsorbate at low adsorbate concentrations, then one can conclude that there is a decreasing number of smaller pores available in the more activated surfaces.

One possible interpretation of these results is that the activation process etches the pores wider, changing the adsorption behavior of these fibers. Kasaoka et al.[20] have activated phenolic fibers to various degrees and examined the aqueous adsorption properties using a number of organic dyes of various geometric sizes in order to determine the molecular sieving behavior of the resulting activated fibers. These researchers found that the fibers did have adsorbate size-dependent adsorption and that fibers of increasing activation allowed progressively larger adsorbates to enter the pores to adsorb. The researchers concluded that the activation process did have the effect of increasing the pore width. This increasing pore width may decrease the number of smaller micropores so important to low concentration adsorption.

What is not clear from the Kasaoka et al. study is the effects that this activation process has on the pore size distribution. One can imagine that the entire distribution is shifted to a greater mean effective pore size perhaps maintaining its shape or possibly developing a skewed distribution. This explanation of increasing pore size agrees with the results presented in this paper. If many of the smaller pores are widened by the activation process, there will be fewer pores to adsorb at low concentrations and more pores to adsorb at higher concentrations. Unfortunately, neither our results nor those of Kasaoka et al. permit any conclusions as to the shape of the micropore distribution, although we can state that with increasing activation duration there are fewer smaller pores and a greater number of larger pores, in the ACF.

We can examine the adsorption behavior numerically with a series of theoretical fibers using the Dubinin–Radushkevich (DR) equation.[11] The DR equation is[32]

$$W = W_0 \exp[-(A/\beta E_0)^2] \quad (1)$$

where

$$A = -\Delta G = RT \ln (P_0/P) \quad (2)$$

In eq 1 W is the volume of adsorbate adsorbed per gram of carbon and W_0 is the total micropore volume (cm^3/g); A is the differential molar work equal to the negative of the differential Gibbs free energy (ΔG); β is a similarity coefficient comparing the characteristic free energies of adsorption for a test and reference vapor, and E_0 is the characteristic adsorption energy for standard vapor (often benzene). In eq 2 P_0 is the saturated adsorption pressure and P is the pressure of interest; R is the universal gas constant and T the absolute adsorption temperature.

The parameters of interest for this equation are W_0 and E_0. We can measure W_0 and Dubinin and Plavnik[33] have shown with a small-angle X-ray scattering technique applied to microporus carbons that the relationship between the slit-pore half-width x_0 and E_0 for a standard vapor benzene at 293 K is given by

$$x_0 = k/E_0 \quad (3)$$

where k is a structural factor in kJ nm/mol and was determined to be 12.0 for x_0 in the range 0.4–1.5 nm.[33]

Equations 2 and 3 can be substituted into eq 1 and plotted three dimensionally as a function of P/P_0, x_0, and cm^3 of adsorption/g of carbon (Figure 8) to show the effect the mean micropore size has on the adsorption isotherm shape. A micropore volume of 0.325 cm^3/g of adsorbent was used for W_0, T was equal to 298 K, β was set to 1.0,

(32) Dubinin, M. M. *Carbon* **1989**, *27*, 457.
(33) Plavnik, G. M.; Dubinin, M. M. *Izv. Akad. Nauk SSSR, Ser. Khim.* **1966**, 620.

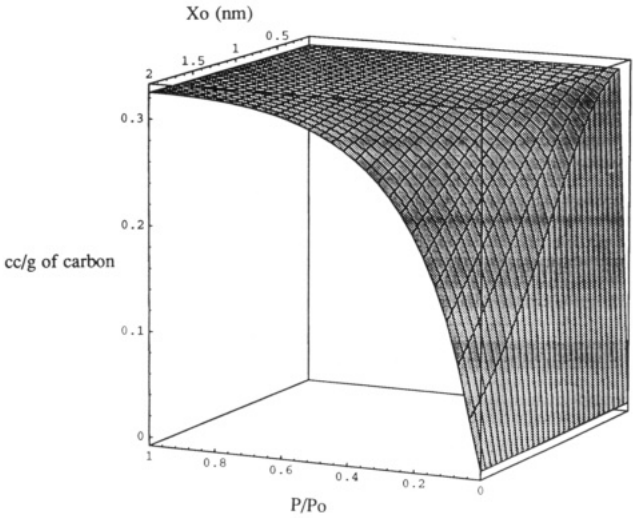

Figure 8. Three-dimensional view of results from Dubinin–Radushkevich equation that describes the adsorption as a function of relative pressure and pore half-width (x_0).

and R was equal to 8.31 J/mol K. The half-width, x_0, was varied from 0.1 to 2.0 nm while P/P_0 was varied from 0 to 1.

In Figure 8 we see that most of the surface is flat and equal to W_0, but as pore dimensions become larger the surface of the plot dips downward at low P/P_0, indicating less adsorbate adsorbed. The larger pores do not benefit from the overlapping adsorption potential of opposite pore walls and thus do not experience the enhanced adsorption observed for the smaller pores.

A set of three theoretical fibers modeled with the DR equation can be used to demonstrate the crossover point observed in the experimental results. Each of the three activated fibers, designated A, B, and C, have a normal distribution of pore sizes but with increasing mean x_0 and W_0. W_0 for each fiber (A, B, C) was chosen to match the experimental micropore volume measured for ACF-15, ACF-20, and ACF-25, respectively, and the constants T, β, and R were set to be the same as in the previous example presented in Figure 8 (i.e., T = 298 K, β = 1, and R = 8.31 J/mol K). The mean x_0 was set to 0.8, 1.3, and 1.6 nm, respectively, for fiber A, B, and C. Substituting these values into eq 1 results in Figure 9, a plot of cm^3 of adsorbate adsorbed/g of fiber as a function of P/P_0.

This figure is similar in shape to that generated experimentally (Figure 5). At low P/P_0 the fiber A, with the lowest value for W_0 and x_0, adsorbs the most at low adsorbate concentrtion but above the crossover point fiber C, with the highest value for W_0 and x_0, adsorbs the most. We cannot presently measure x_0 but are setting up instrumentation to determine the mean x_0 of the ACF samples with argon and nitrogen at their respective boiling points. This will allow us to compare the experimental and theoretical results quantitatively.

It is important to recognize that materials designed for the removal of VOC in low concentration environments require the adsorbent to have numerous and as narrow of micropores as possible while still allowing the molecules into the pores. Surface area or its resulting effective pore volume alone is not an adequate design parameter. The micropore size and its distribution are the important parameters.

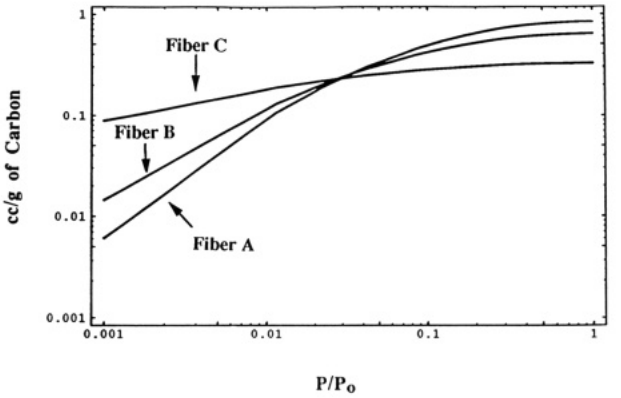

Figure 9. Adsorption properties of three theoretical fibers as a function of the relative pressure using the Dubinin–Radushkevich equation. Pore volume and mean pore size are different for each fiber.

Summary and Conclusions

Effective pore volume of these fibers was determined with the adsorption of an individual VOC saturated in nitrogen and was found to increase with duration of activation as expected. In contrast, at low adsorbate concentrations, the amount of equilibrium adsorption of *n*-butane (49.8 ppmv), acetone (10.3 ppmv), and benzene (56.5 ppmv) in nitrogen or air was found to decrease with increasing duration of activation. That is, at low concentrations, ACF with the least pore volume adsorbed the greatest amount of adsorbate. This could be explained by a micropore filling process where the smaller micropores are preferentially filled at lower concentrations. It was concluded that the fibers with least activation had a greater volume of small width micropores than the highly activated fibers. It is hypothesized that the duration of activation acts to enlarge the micropores shifting the distribution of pores to higher mean pore sizes.

This hypothesis of the relationship between activation and pore size was further demonstrated with the Dubinin–Radushkevich equation. With a series of three theoretical fibers with both increasing mean micropore half-width (x_0) and total pore volume (W_0) the resulting adsorption isotherm was qualitatively similar to the experimental adsorption isotherm observed with *n*-butane including the crossover point.

Characterizing the shape of the micropore distribution and learning how to control it during activation is critical to the optimization of these materials for a variety of adsorption applications including maintaining and improving ambient air quality. These studies are currently underway along with evaluating the effect of chemically modifying the carbon surface.

Acknowledgment. We thank the Center for Indoor Air Quality (CIAR) for funding this research. We also would like to thank Joe Hayes of American Kynol Inc. for his discussions and for providing the activated carbon fibers. XPS and SEM analysis was carried out in the Center for Microanalysis of Materials, University of Illinois, which is supported by the U.S. Department of Energy under Contract DEFG02-91-ER45439.

Registry No. $CH_3C(O)CH_3$, 67-64-1; cyclo-C_6H_{12}, 110-82-7; C_6H_6, 71-43-2; $C_6H_5CH_3$, 108-88-3; CH_3CCl_3, 71-55-6; $CH_3(CH_2)_2CH_3$, 106-97-8.